

# A focused electric spark source for non-contact stress wave excitation in solids

Xiaowei Dai and Jinying Zhu<sup>a)</sup>

*Department of Civil, Architectural and Environmental Engineering, The University of Texas at Austin, Austin, Texas 78712*  
*xdai@utexas.edu, jyzhu@mail.utexas.edu*

Michael R. Haberman

*Applied Research Laboratories, The University of Texas at Austin, P.O. Box 8029, Austin, Texas 78713-8029*  
*haberman@arlut.utexas.edu*

**Abstract:** A focused electric spark is used as a non-contact acoustic source to excite stress waves in solids. The source consists of an electric spark source located at the near focus of an ellipsoidal reflector that focuses the acoustic disturbance generated by the spark source to the far focal point. Experimental studies using both contact and non-contact sensors indicate that the source has the capability to excite the Rayleigh surface wave and impact-echo mode (S1-zero-group-velocity Lamb mode) in a 250 mm thick concrete slab and to enable fully air-coupled testing of concrete specimens.

© 2013 Acoustical Society of America

PACS numbers: 43.40.Yq, 43.20.Ye, 43.35.Pt [JM]

Date Received: June 29, 2013      Date Accepted: October 9, 2013

## 1. Introduction

Historically, electrical sparks in air have been used as an acoustic source for the study of nonlinear acoustic waves (Wright and Medendorp, 1968) and as a sound source for impulse response measurement in architectural acoustics (Cann and Lyon, 1979). Since the 1990s, a few studies have also reported the use of spark sources for elastic wave generation in solids with limited success (Korolev *et al.*, 1987; Korolev and Krylov, 1988). High energy spark generators produce high amplitude  $N$  waves in air due to the rapid heating and subsequent expansion of the gas after the breakdown voltage is reached (Wright and Medendorp, 1968). The acoustic wave front is cylindrical in the near field but transitions to a spherically diverging wave at distances on the order of the source length, which is the gap between the electrodes (Korolev and Krylov, 1990). The electrical spark is also adopted in the electrohydraulic (EH) type lithotripters (Coleman and Saunders, 1989), which employ an ellipsoidal reflector to redirect an acoustic disturbance resulting from an underwater electrical discharge centered at the near focus to amplify the acoustic level at the far focus. In the case of lithotripsy, the system is immersed in water to facilitate energy transmission to the body. In this paper, the authors report research on an in-air focused spark system inspired by lithotripters to be used as a non-contact air-coupled source for ultrasonic excitation of stress waves in elastic media. This work demonstrates that despite the large acoustic impedance mismatch at the air-solid interface, the elevated pressure amplitude of the focused acoustical disturbance provides sufficient energy to enable air-coupled ultrasonic excitation in solids.

The impact echo (IE) method for nondestructive testing (NDT) of concrete is chosen to demonstrate the feasibility of the non-contact acoustic source reported here.

---

<sup>a)</sup> Author to whom correspondence should be addressed.

Since the IE test was developed in 1980s (Sansalone and Carino, 1986), it has become a common NDT technique to determine thickness of plates and to locate delaminations. Theoretical analyses indicates that, for isotropic plates, the IE resonance vibration mode corresponds to the non-propagating, zero-group-velocity,  $S_1$  Lamb wave mode ( $S_1$ ZGV) (Gibson and Popovics, 2005; Holland and Chimenti, 2003). The IE resonance frequency,  $f_{IE}$ , is related to the thickness of plate  $H$  and P-wave velocity  $V_P$  by the equation  $f_{IE} = \beta V_P/H$ , where  $\beta$  is dimensionless parameter close to 1 that depends on the Poisson's ratio of material. For concrete,  $\beta$  varies between 0.94 and 0.96.

Most stress wave based NDT methods require contact between sensors and test surface. The contact requirement significantly limits test speed and is one of the major challenges in NDT of large infrastructure. Development in air-coupled sensing for concrete (Zhu and Popovics, 2007; Dai *et al.*, 2011) provides a partial solution for rapid scanning of concrete structures and more consistent signals by employing air-coupled sensors (microphones) and a contact impact source for wave excitation. However, to make a true breakthrough in rapid scanning, a non-contact air-coupled source is required to realize a fully air-coupled testing system. A recent study (Abraham *et al.*, 2012) demonstrates feasibility of fully air-coupled surface wave velocity measurement on near surface layer of concrete. The ultrasonic frequencies used for NDT of concrete are usually below 100 kHz to avoid strong scattering by aggregates. However, most commercially available air-coupled ultrasonic systems employ focused, narrow-band, high frequency transducers (Grandia and Fortunko, 1995), with the limitation of operating only at a few pre-selected frequencies ranging from 50 kHz to 4 MHz.

As an alternative to existing air-coupled transducers, a high power electrical spark source with accompanying ellipsoidal reflector is proposed here to excite stress waves in elastic solids. The electrodes of the spark generator are positioned at the near focus of the reflector and the far focus is aligned with the test surface. A fully air-coupled test setup was used to measure Rayleigh and IE mode responses on concrete. Contact measurements are also shown for comparison. It is further demonstrated that the IE mode can be measured from the back side of the plate using through transmission setup.

## 2. Experimental demonstration

### 2.1 Experimental setup

The spark source includes two major components: a spark generator and an ellipsoidal reflector. In this test, a GTS-51 spark generator made by Grozier Technical Systems Inc. was used to generate electric sparks between two electrodes, separated by an air gap, which are located at the focus of an aluminum ellipsoidal reflector. The reflector has a major axis  $2a = 280$  mm, minor axis  $2b = 140$  mm, and eccentricity of 0.866. The depth of reflector is 259 mm, and the bottom surface is 2 mm above the far focus. The reflector is supported by a frame to align the far focus plane with the test surface. The concrete specimen has dimensions of 1500 mm  $\times$  1500 mm  $\times$  250 mm and a measured P-wave velocity and Poisson's ratio of 4086 m/s and 0.22, respectively. Figure 1 shows the picture of the ellipsoidal reflector [Fig. 1(b)].

The four test setups investigated in the study are summarized in Fig. 1(a). The first two setups position the spark source and the sensors on the same side of the plate. In the first setup, two accelerometers (PCB 352C65) with 20 cm spacing were aligned with the spark source. This setup was used for both surface wave and IE measurements. Though the objective of this study is ultimately to enable fully air-coupled NDT of concrete slabs, contact sensors were used as benchmark measurements that validate the existence of Rayleigh and IE mode wave motion at the concrete-air interface. The second setup was fully air-coupled, employing two microphones (PCB 377A01) in place of the accelerometers. To reduce acoustic self-noise in the system, each microphone was enclosed by an external sound insulation cylinder

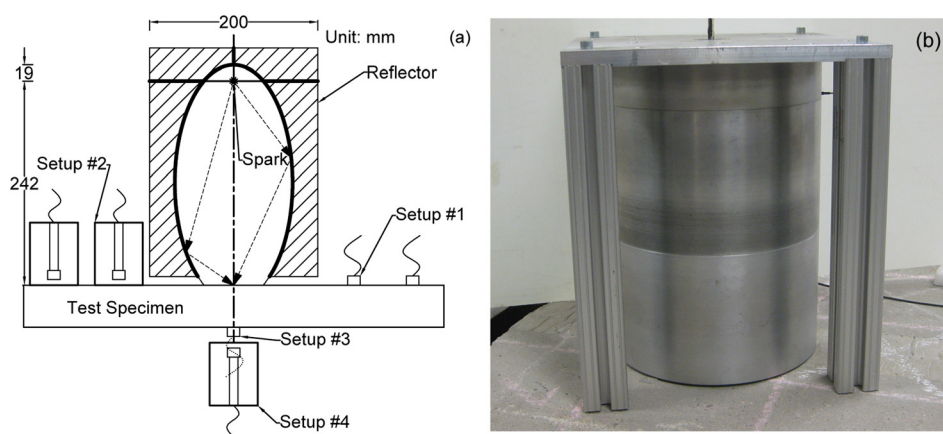


Fig. 1. (Color online) (a) Four test setups using the air-coupled spark source on a 250 mm thick concrete slab. (b) The ellipsoidal reflector used to focus a spark source.

(Zhu and Popovics, 2007). In the third and fourth setups, the sensors were placed on the opposite side of the plate, measuring the through transmission signals. Signals were digitized by a digital oscilloscope NI USB 5133 at 1 MHz.

## 2.2 Characterization of the spark source

To characterize the focusing gain from the ellipsoidal reflector, a hydrophone was used to measure the in-air on-axis pressure at the far-focus of the reflector. Those results were then compared to measurements of the on-axis pressure at 242 mm from the spark without the reflector present to estimate the signal gain resulting from the presence of the focusing reflector. A hydrophone (Brüel & Kjær type 8103) was employed in place of a microphone because the high amplitude of focused pressure ( $> 150$  dB) will overload most microphones. The hydrophone has a nominal sensitivity of  $26.3 \mu\text{V}/\text{Pa}$  and  $\pm 1.8$  dB accuracy from 0.1 Hz to 100 kHz. Since the hydrophone is designed for measurements in water, the actual sensitivity and bandwidth in air may be different. Therefore, the in-air sensitivity of the hydrophone was approximately measured by comparing its response to that of an equidistant GRAS 40BE microphone (4 mV/Pa,  $\pm 3$  dB in 4 Hz to 100 kHz) when excited by sparks located in an anechoic chamber. For the spark-receiver spacing ranging from 0.3 to 1.5 m, the responses from the hydrophone and the microphone are shown in Fig. 2(d). These measurements indicate that the pressure measured by the hydrophone is about 14 dB lower than that measured by the GRAS microphone in the frequency range of interest. Therefore, the peak pressure at the focal point can be estimated by applying 14 dB correction to the hydrophone measurement. The B&K 8103 hydrophone enabled the measurement of the approximate pressure signal at the focus of the transducer which would have been impossible with most standard microphones.

As shown in Fig. 2(b), the pressure signal measured at the reflector focus has significantly higher amplitude than that of the direct spark wave in Fig. 2(a). Meanwhile, the direct wave component is also observed in the focused signal before the focused wave arrival since it travels a shorter path. The amplitude spectra in Fig. 2(c) show that the ellipsoidal reflector provides a maximum gain of 31 dB around 10 kHz. It should be noted that the actual bandwidth of spark source may be broader, because the measured signal is limited by the bandwidth and response time of the hydrophone. Further, the ellipsoidal reflector forms a focal zone in the region of the focal point. Figure 2(d) show the peak pressure values measured along the axis of reflector by the B&K hydrophone and the GRAS microphone, with the origin located at the far focus. The largest pressure measured by the hydrophone occurs at the focal

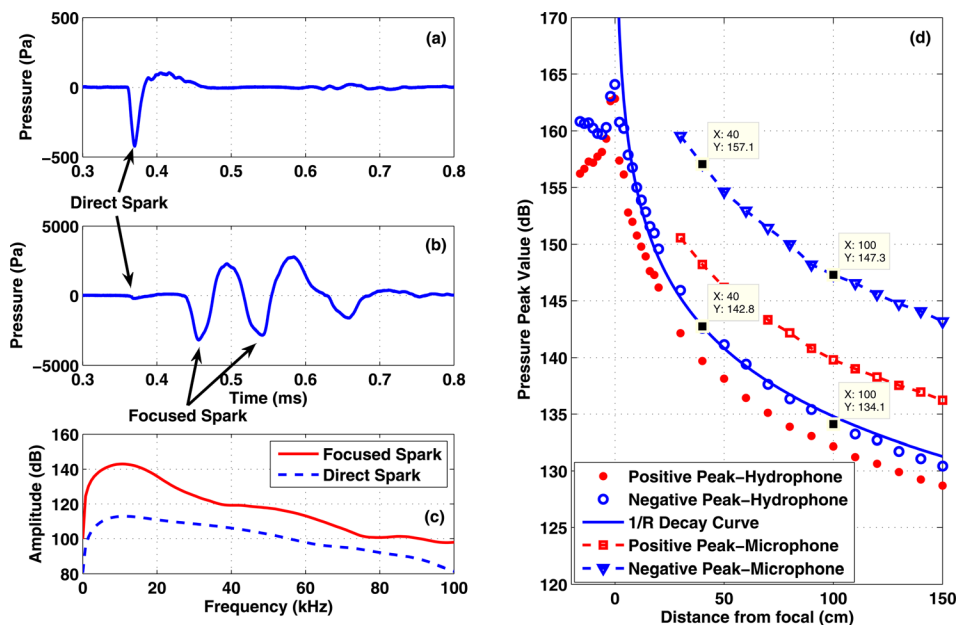


Fig. 2. (Color online) Time domain pressure signals measured (a) at 242 mm from the spark without a reflector, (b) at the far focus of the ellipsoidal reflector. A comparison of the spectra from these two signals is shown in (c). The peak pressure curves along the reflector axis measured by the B&J hydrophone and the GRAS microphone are shown in (d). Negative distance indicates the measuring point is inside the reflector.

point with a peak pressure of 164 dB. Applying the 14 dB pressure correction to the hydrophone measurement, the peak pressure at the focus is estimated as 178 dB. In addition, the peak pressure decays with distance approximately at the rate of  $1/r$  when the distance is larger than 10 cm.

### 2.3 Rayleigh surface wave measurement

A transient point force is effective for generating Rayleigh surface wave in solid media. Two sensors aligned with the source point are used in Rayleigh wave velocity measurement. The velocity can be estimated in time domain signals by picking the arrival times on each signal, or they can be determined in frequency domain using the spectral analysis of surface waves (SASW) method (Nazarian *et al.*, 1983).

Figures 3(a) and 3(b) show signals measured by two accelerometers (setup #1) and Figs. 3(c) and 3(d) show signals measured by two microphones (setup #2), respectively. The arrival times of Rayleigh waves generated by the direct spark and the focused spark are marked in the figure. Since the direct spark wave propagates directly from the spark to the test surface without reflection, its propagation path is shorter than the path of the focused spark wave by  $2a(1-e)$ , where  $a$  is the semi-major axis and  $e$  is the eccentricity of the ellipse. For the reflector used in this study, the difference in travel distance is 38 mm, which results in a 1.1 ms delay for the sound wave traveling through air. In Fig. 3(a), it is clearly shown that the arrival time of the Rayleigh wave generated by the focused spark has 1.1 ms delay compared with the one generated by the direct spark. With the accelerometer spacing of 20 cm, and the Rayleigh wave time delay between the two sensors 0.089 ms, the calculated Rayleigh wave velocity is 2247 m/s, which agrees with measurements on the specimen using a contact source and contact sensors.

The two microphone signals shown in Figs. 3(c) and 3(d) have a 0.095 ms time delay, which leads to Rayleigh wave velocity of 2105 m/s, slightly slower than the value measured by accelerometers. The measurement error is mainly caused by the height difference between the two microphones, which can be eliminated by repeating the test

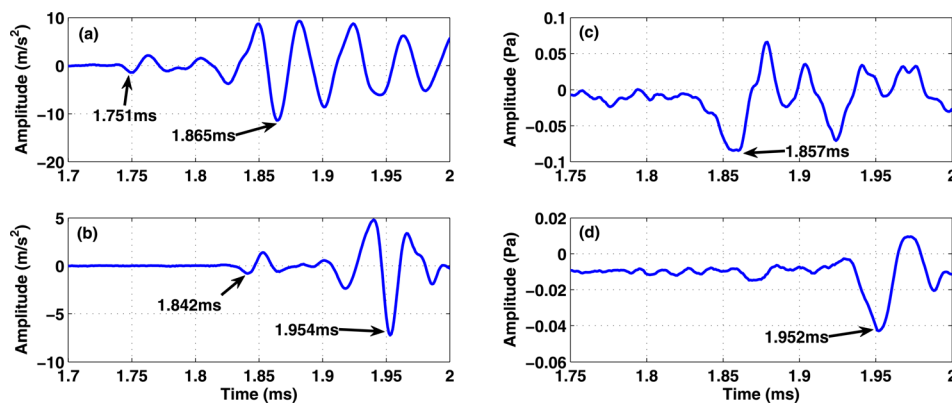


Fig. 3. (Color online) Time domain signals measured by the accelerometers (a) and (b); and by the microphones (c) and (d) with 20 cm spacing. The arrival times of the Rayleigh wave generated by the direct spark and the focused spark are marked on the waveform.

and placing the spark source on the left side of the sensors. This method has been adopted to reduce inconsistency caused by sources and coupling conditions (Kee and Zhu, 2010).

2.4 *S<sub>1</sub>ZGV Lamb mode (Impact-echo)*

The sensor configurations described above can also be used to measure the *S<sub>1</sub>ZGV* Lamb wave mode excited by the spark source. Signals are analyzed in frequency domain to identify the peak frequency associated with this resonance mode. The amplitude spectra of signals measured by an accelerometer and a microphone are shown in Figs. 4(a) and 4(b), respectively. Both signals show largest peaks around 9.8–9.9 kHz, which agree with measurements using a contact source. To reduce the airborne acoustic noise generated by the speak source, the air gap between the reflector and concrete surface was sealed with silicon tape in this study. Although it is unrealistic to seal the gap in practice, this test demonstrates the feasibility to excite the *S<sub>1</sub>ZGV* Lamb mode (IE mode) in a concrete plate using the spark source. The authors are currently investigating noise insulation/reduction measures to reduce the effect of acoustic noise.

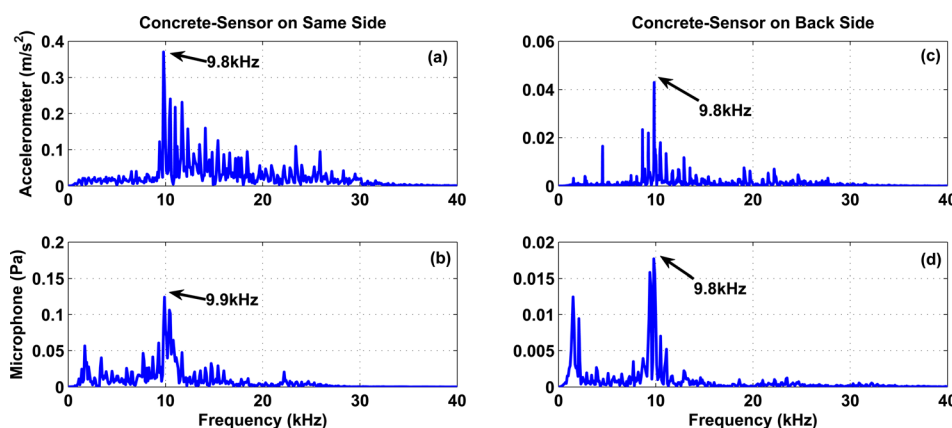


Fig. 4. (Color online) Amplitude spectra of *S<sub>1</sub>ZGV* Lamb wave mode signals measured on the concrete plate, by an accelerometer (the top row) and by a microphone (the bottom row). The receiver is located on the same side as the spark source in (a) and (b) and the back side of specimen in (c) and (d).



### 2.5 Through transmission measurement

When the spark source and receivers are located on the same side of test specimen, strong acoustic self-noise generated by the spark may mask stress wave signals radiated from the surface of the solid, especially in the fully air-coupled setup when microphones are used as receivers. In Fig. 4(b), the signal was obtained when the gap between the reflector and test plate was sealed to reduce the noise level. In a through transmission test configuration, however, the test specimen serves as a sound barrier to block acoustic self-noise. In test setups #3 and #4, the  $S_1ZGV$  Lamb wave mode was measured on the back side of the plate using an accelerometer and a microphone. The amplitude spectra for both signals are shown in Figs. 4(c) and 4(d). Both measurements show the correct frequency for the expected  $S_1ZGV$  Lamb mode, which can be used to determine the P wave velocity of material or to detect defects in the plate. In time-of-flight based ultrasonic tests, to obtain consistent wave transmit time, it is necessary to maintain strict alignment between the source and receiver and keep accurate lift-off distance between the sensor and test surface. However, the  $S_1ZGV$  mode is a non-propagating Lamb wave mode, with a mode shape of Bessel function (Gibson and Popovics, 2005). The  $S_1ZGV$  frequency can be measured even at a large source-receiver offset distance (up to 90 cm) with a large lift-off height (up to 50 cm) (Dai *et al.*, 2011). Therefore, the resonance frequency measurement is not affected by small misalignments or variation of the lift-off distance between the source and the sensor. The Ultrasonic Pulse Velocity (UPV) test based on P wave through transmission measurement is one of the most common NDT methods for concrete structures. The air-coupled test system in setup #4 demonstrates a fully non-contact ultrasonic test as an alternative to UPV tests for rapid NDT scanning of concrete structures.

### 3. Discussion and conclusions

In this paper a low cost and efficient air-coupled source is presented for stress wave excitation in NDT of solids. An ellipsoidal reflector is used to focus the outgoing pressure wave generated by an electrical spark discharge onto the surface of an elastic solid collocated with far focus of the reflector. Experimental studies reported here show that the focused spark source is able to generate pressures of sufficient amplitude to permit Rayleigh and  $S_1ZGV$  mode Lamb wave mode measurements using a fully air-coupled setup. Using a through transmission configuration, the spark source provides a solution to fully non-contact, rapid NDT of plate structures made from high impedance elastic solids.

### Acknowledgments

This work was supported by a subcontract from Rutgers University, under the support of National Institute of Standards and Technology, Technology Innovation Program, Cooperative Agreement No. 70NANB10H014.

### References and links

- Abraham, O., Piwakowski, B., Villain, G., and Durand, O. (2012). "Non-contact, automated surface wave measurements for the mechanical characterisation of concrete," *Constr. Build. Mater.* **37**, 904–915.
- Cann, R. G., and Lyon, R. H. (1979). "Acoustical impulse response of interior spaces," *J. Audio Eng. Soc.* **27**(12), 960–964.
- Coleman, A. J., and Saunders, J. E. (1989). "A survey of the acoustic output of commercial extracorporeal shock wave lithotripters," *Ultrasound Med. Biol.* **15**, 213–227.
- Dai, X., Zhu, J., Tsai, Y., and Haberman, M. R. (2011). "Use of parabolic reflector to amplify in-air signals generated during impact-echo testing," *J. Acoustic. Soc. Am.* **130**, EL167–EL172.
- Gibson, A., and Popovics, J. S. (2005). "Lamb wave basis for impact-echo method analysis," *J. Eng. Mech.* **131**, 438–443.
- Grandia, W. A., and Fortunko, C. M. (1995). "NDE applications of air-coupled ultrasonic transducers," *Ultrasonics Symp.* **1**, 697–710.

- Holland, S. D., and Chimenti, D. E. (2003). "Air-coupled acoustic imaging with zero-group-velocity Lamb modes," *Appl. Phys. Lett.* **83**, 2704–2706.
- Kee, S.-H., and Zhu, J. (2010). "Using air-coupled sensors to determine the depth of a surface-breaking crack in concrete," *J. Acoust. Soc. Am.* **127**, 1279–1287.
- Korolev, S. V., Krasilnikov, V. A., and Krylov, V. V. (1987). "Mechanism of sound generation in a solid by a spark discharge near the surface," *Sov. Phys. Acoust.* **33**, 451–452.
- Korolev, S. V., and Krylov, V. V. (1988). "Efficient excitation of Rayleigh waves by a strong shock wave initiated by a spark in air," *Sov. Tech. Phys. Lett.* **14**, 843–845.
- Korolev, S. V., and Krylov, V. V. (1990). "Directivity patterns of a spark source of acoustic waves in a solid," *Sov. Phys. Acoust.* **36**, 21–24.
- Nazarian, S., Stokoe, K. H. II, and Hudson, W. R. (1983). "Use of spectral analysis of surface waves method for determination of moduli and thicknesses of pavement systems," *Transport. Res. Rec.* **930**, 38–45.
- Sansalone, M. J., and Carino, N. J. (1986). *Impact-echo: A Method for Flaw Detection in Concrete Using Transient Stress Waves* (National Bureau of Standards, Gaithersburg, MD).
- Wright, W. M., and Medendorp, N. W. (1968). "Acoustic radiation from a finite line source with N-wave excitation," *J. Acoust. Soc. Am.* **43**, 966–971.
- Zhu, J., and Popovics, J. S. (2007). "Imaging concrete structures using air-coupled impact-echo," *J. Eng. Mech.* **133**, 628–640.